On the trustworthiness of a digital 3D MEMS gyroscope responsiveness to dynamic accelerations for ADAS applications

This is the author's accepted version of the contribution published as:

Original
On the trustworthiness of a digital 3D MEMS gyroscope responsiveness to dynamic accelerations for ADAS applications / Schiavi, Alessandro; Iacomussi, Paola; Rossi, Laura; Prato, Andrea; Mazzoleni, Fabrizio; Facello, Alessio; Genta, Gianfranco; Signoretti, Raffaele. - (2021), pp. 70-75. (Intervento presentato al convegno 2021 IEEE International Workshop on Metrology for Automotive (MetroAutomotive) tenutosi a virtual conference nel 1-2 July, 2021) [10.1109/MetroAutomotive50197.2021.9502726].
Availability:
This version is available at: 11696/71022 since: 2023-05-31T15:10:16Z

Publisher:
IEEE

Published
DOI:10.1109/MetroAutomotive50197.2021.9502726

(Article begins on next page)

On the trustworthiness of a digital 3D MEMS gyroscope responsiveness to dynamic accelerations for ADAS applications

Alessandro Schiavi
Applied Metrology and Engineering
INRiM –National Institute of Metrological Research Turin, Italy a.schiavi@inrim.it

Paola Iacomussi
Applied Metrology and Engineering
INRiM –National Institute of Metrological Research Turin, Italy
p.iacomussi@inrim.it

Laura Rossi
Technology Center Engineering Excellence
Altran, Italy
Turin, Italy laura.rossi@altran.it

Andrea Prato
Applied Metrology and Engineering
INRiM –National Institute of Metrological Research Turin, Italy
a.prato@inrim.it

Fabrizio Mazzoleni
Applied Metrology and Engineering
INRiM –National Institute of
Metrological Research Turin, Italy f.mazzoleni@inrim.it

Alessio Facello
Applied Metrology and Engineering
INRiM –National Institute of
Metrological Research Turin, Italy a.facello@inrim.it

Gianfranco Genta
Department of Management and Production Engineering Politecnico di Torino
Turin, Italy gianfranco.genta@polito.it

Raffaele Signoretti
Motor Vehicle Engineering Mechanical Engineering
Politecnico di Torino
Turin, Italy s237833@studenti.polito.it

***Abstract*— In recent years, the development of advanced driver assistance systems (ADAS) up to fully automated vehicles (AV), based on digitalization and boosted big data managing within dense multi-sensor networks, has become a strategic perspective for automotive and mechatronics engineering, oriented toward innovation of transports, infrastructure-vehicle and vehicle-to- vehicle real-time interconnections, automation in transport systems for people and goods and in smart farming, including safety-driving, navigation and positioning systems, traffic flows management and pollution controls. One of the key points for the development of safe and trustworthy ADAS and AV systems is linked to the accuracy and the reliability of sensors employed in multi-sensor networks, thus on traceable metrological characterizations, based on standard procedures and/or experimental methods widely agreed. In this work, the trustworthiness, in terms of data output reliability, stability and accuracy, of a digital 3D gyroscope integrated into a commercial multisensory MEMS, subjected to external vibrations, is investigated. The sensor is mounted on inclined planes (6 tilted angles, between 0° and 90°) andat 8 different rotation angles (from 0° to 360°); the inclinedplanes are fixed on a vibrating table. The static condition, as a function of tilt and rotation, is preliminarily investigated in the local gravitational field. Dynamic conditions are investigated by generating a sinusoidal horizontal acceleration, at a nearly-constant amplitude of 0.1 m s^{-2} at 2 Hz, along the horizontal direction for 120 s. Both static and dynamic reference accelerations are traceable to the absolute gravimetry, and the vibration primary standard, at INRIM.**

Keywords*—*3D MEMS gyros, dynamic analysis, trustworthiness, reliability, traceability

I. INTRODUCTION

Vehicular automation, in the broadest meaning of the terms, as well as being very attractive for many practical advantages, ranging e.g., from safety to traffic flows management, still present severalconcerns [1 – 2]. Many automotive industries are carrying on studies, research and developments in the field of smart mobility and automation (from partial automation L2, up to high L4 or full automation L5), but as is known, progresses are slowed down by severaltechnical difficulties, mainly linked to the managing of unpredictable events, such as the human-car interaction or weather conditions, the reliability of fast-real-time hardware-software communications, the control of sensors malfunctioning, and data quality assessment to manage safe operations in autonomous decision making. The trustworthiness of the whole complex multi-sensing infrastructure integrated into vehicles is a fundamental requirement not only for safe and reliable development of vehicular automation, and for the consequently enhanced quality of the product, but also for several legal and insurance reasons, within smart mobility perspectives worldwide [3 – 4].

A trustworthy automation systemis founded on the inherent reliability of its components, elements, and interconnected sensors, and on the quality of data acquired, transferred, processed, stored and distributed. The knowledge of metrological attributes, such as accuracy, precision and traceability of sensors interfacing with the physical world and environment, allows improving the quality of data provided, with information on uncertainties, confidence levels, traceabilityand sensitivity, supplied by calibration procedures and metrological characterizations.

By referring to the International Vocabulary of Metrology (VIM) [5], accuracy is related to the closeness of agreement between a measured quantity value and the reference value (e.g., a «true value», or physicalquantity); the precision quantifies the width of data dispersion (scattering of data) of the measured quantity value; the traceability relies upon an unbroken chain of comparisons to stated reference values each with a declared uncertainty, within the International System of Units (SI); and the sensitivity is defined as the ratio between the indication provided by the sensor and the corresponding value of the reference value. In Figure 1 a schematic representation of metrological attributes is depicted.

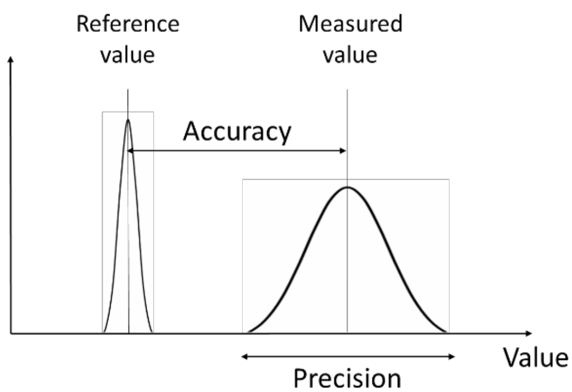

Figure 1. Representation of metrological attributes.

The above-mentioned metrological attributes are generally provided (and available in issued calibration certificate) for measuring instruments or devices, conceived to measure physicalquantities, but they could also be provided for sensors, designed to detect (or "perceive") the variations/characteristics of the surrounding environment. It follows that a calibrated sensor allows providing trustworthy information of the physical world detected, based on data accuracy and precision. The trustworthiness of data [6], provided by sensors integrated into vehicles, has high potential in the development of high quality and safety automation, improving the technical performance of advanced driver assistance systems (ADAS) and automated vehicles (AV).

This paper investigates the trustworthiness of a digital 3D MEMS gyroscope for ADAS applications, when subjected to dynamic accelerations, based on a proper metrological characterization. As it is known, gyroscopes, combined with accelerometers, are the basic components of inertial measurement units (IMUs), integrated into vehicles to detect amplitude and direction of the acting forces, the angular rate, and the orientation. Recently, based on proper calibration procedures nowadays available, the metrological traceability of digital 3-axis MEMS accelerometers can be provided, for both inertial and dynamic conditions, with the proper accuracy and precision, from traceability and detailed uncertainty budgets [7, 8]. Nevertheless, the accuracy and the precision of angular rate data, in dynamic conditions (i.e., in strong vibrating environments, such as a vehicle in motion on a damaged road) was not fully investigated and several lacks related to the mechanical behavior are still unknown.

III. MATERIALS ANS METHODS

A. *Inertial measurement units (IMUs) in vehicles*

Basically, IMU integrated into vehicles is a 6 degrees-of- freedom sensor able to control simultaneously 3D accelerations, along with vertical and horizontal directions (i.e., surge, sway and heave), and 3D angular rate, around the same directions (i.e., roll, pitch, and yaw), as schematically shown in Figure 2.

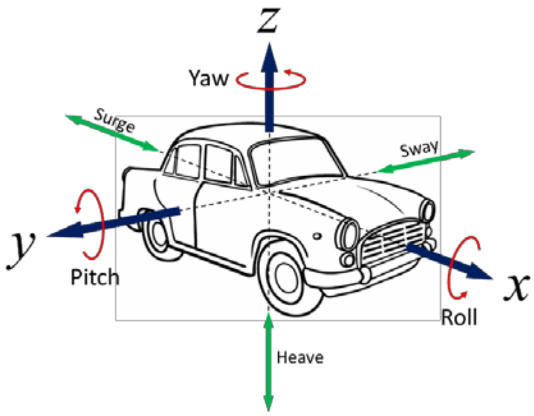

Figure 2. Dynamic movements of a vehicle, along with vertical and horizontal directions.

IMU monitors the dynamic changes in the movements of a vehicle and it is the main component of the sensing infrastructure related to stability, control, and positioning, allowing to make safe decisions in the place of a human operator. Moreover, dynamic data provided by the IMU, combined with maps and "*perception stack*" data, provide information about objects and features around the vehicle.

B. *IMU under investigation*

The IMU investigated in this work, is a commercial low- power digital 3D accelerometer and 3D gyroscope (ST, model LSM6DSR [9]), that generates acceleration and angular rate output data, working as a combo accelerometer-gyroscope sensor. The IMU is composed of high-performance 3-axis digital accelerometer and 3-axis digital gyroscope sensors, a power supply, a charge amplifier, and an analog-to-digital converter, connected by a serial cable to a separated external microcontroller (ST, model 32F769IDISCOVERY [10]), to acquire digital data and to provide the required power supply and clock to the MEMS accelerometer and gyroscope. The signal is acquired through a Serial Peripheral Interface (SPI), which is a synchronous serial communication interface used for connecting digital sensors. The 1-bit signal from the ΣΔ-ADC is then converted through a decimation process and a low pass filter into a standard 16-bit-signed PCM (Pulse Code Modulation) signal with nominal sampling frequency rates ranging from 12.5 Hz up to 6.6 kHz. According to the imposed full scale, linear acceleration sensitivity ranges from 0.061 m*g*/LSB to 0.488 m*g*/LSB, and angular rate sensitivity ranges from 4.375 mdps/LSB and 140 mdps/LSB, where LSB is the acronym for Least Significant Bit.

As introduced in previous works [11 – 15], to provide the proper metrological attributes, the sensitivity is expressed in terms of «digitized sensitivity» $D_{n\text{-bit}}/\mathrm{m{\cdot}s^{-2}}$ (optionally $D_{n\text{-bit}}/g$) for acceleration, and $D_{n\text{-bit}}/\mathrm{rad{\cdot}s^{-1}}$ (optionally $D_{n\text{-bit}}/\mathrm{deg{\cdot}s^{-1}}$) for angular rate, where $D_{n\text{-bit}}$ is the decimal-converted *n*-bit-string of the PCM signal (indication of the IMU), to be correlated to the reference physical quantity, in this case, acceleration in m/s^2 and angular rate in rad·s^{-1}, and to the SI.

The amplitude values of IMU range between $-2^{16-1}=-32768$ $D_{16\text{-bit-signed}}$ and $+(2^{16-1}-1)$ $=+32767$ $D_{16\text{-bit-signed}}$, where the digit unit is a signed 16-bit sequence converted into a decimal number. Thus, in the following, the measured «digitized sensitivity» of DUTs is expressed in terms of $D_{16\text{-bit}}/(\mathrm{m{\cdot}s^{-2}})$, and $D_{16\text{-bit}}/(\mathrm{rad{\cdot}s^{-1}})$, in analogy to the typical sensitivity of analog sensors.

The digitized sensitivity is not in conflict with the «adjusted sensitivity» provided by manufacturers, expressed in terms of Least Significant Bit (LSB) related to the physical reference value, i.e., *g*/LSB or dps/LSB, as commonly used according to IEEE Standard, but it represents a further quality parameter of the IMU, allowing to provide the accuracy of measurements, with reference to the static and dynamic calibration. In this particular case, 1 LSB is equal to 1 $D_{16\text{-bit-signed}}$.

C. *Calibration system and procedure*

The calibration system consists of a set of 6 stiff inclined planes (with an inclination of 0°, 15°, 35°, 55°, 75°, and 90°, with respect to horizontal axis), combined with a vibrating table (*PCB Precision Air Bearing Calibration Shaker*). On the inclined planes, 8 prefixed rotational positions are allowable (with a rotation of 0°, 45°, 90°, 135°, 180°, 225°, 270°, and 315°) on which the IMU under investigation is located. In Figure 3, the geometrical principle of the method, and the actual inclined plane, on which the IMU is fixed during calibration on the vibrating table, is shown:

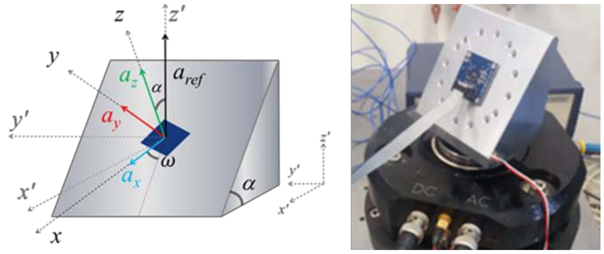

Figure 3. Inclined plane– 3-D scheme and the calibration set-up: the MEMS is fixed to the inclined plane on the vibrating table.

Inclined planes and rotational positions (realized with numerical control machines with a tolerance of ± 0.1◦), allow generating a projection of the gravity acceleration g_{abs} along three axes simultaneously [7]. The reference acceleration due to gravity g_{abs} is measured by the INRiM absolute rise-and-fall gravimeter, namely g_{abs} = (980 534 196.8±8.7)×10^{-8} m·s^{-2}. The alignment of the gravitational field, with respect to the IMU axes, is adjusted by an engineer's spirit level (0.05 mm/m) [16, 17]. In this way, the off-set due to the gravitational field is investigated for the 3 sensitive axes at 4 positions, and the occurring angular rates are expected to be zero (or negligible within electrical noise).

From trigonometrical laws, according to this calibration set- up, the reference gravity accelerations detected by the IMU along its three sensitive axes, are:

$$g_x = | g_{abs} \sin(\alpha)\cos(\omega)| \quad (1)$$

$$g_y = | g_{abs} \sin(\alpha)\sin(\omega)| \quad (2)$$

$$g_z = | g_{abs} \cos(\alpha)| \quad (3)$$

where, α is the inclination angle, ω is the angle of rotation, g_{abs} is the reference acceleration due to gravity along the vertical axis *z'* of the system, and g_x, g_y, g_z are the values of the reference accelerations spread along *x*-, *y*- and *z*-axis of the IMU accelerometer, respectively.

D. Metrological characterization

Once the off-set due to the gravitational field along the three sensitivity axes of IMU for the 4 configurations is determined, in inertial conditions, the response in dynamic conditions is investigated. A single horizontal sinusoidal acceleration a_{ref} is generated along the horizontal axes of the system(perpendicular to *g*). The nearly-constant amplitude of 1 m s^{-2} at 2 Hz acts as a vibrating environment. Since no variations of angle position are imposed to the IMU, the angular rate detected is expected to be nearly zero, also in dynamic conditions, and the acceleration due to gravity along the three axes is expected to be constant with frequency.

IV. Experimental Results

A. Static conditions

The experimental values of the reference gravity accelerations spread along *x*-, *y*- and *z*-axis of the IMU, g_x, g_y, g_z in static conditions, are determined for the 48 configurations according to relations (1)-(3), and expressed as the respective average values and expanded uncertanties, from statistical analysis. By way of example, in the following graphs, from Figure 4 to Figure 6, the resulting indications of the 3D gravity offset, the 3D angles and the 3D gyroscope, are depicted, for the configuration with inclination α = 75°, at ω = 315° of rotation.

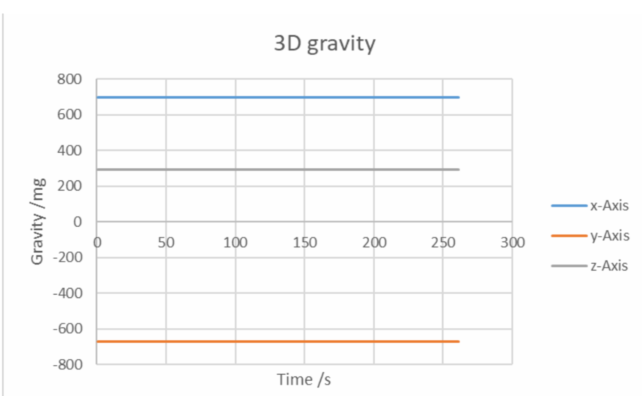

Figure 4. The 3D gravity offset, spreaded along *x*-, *y*- and *z*-axis of the IMU.

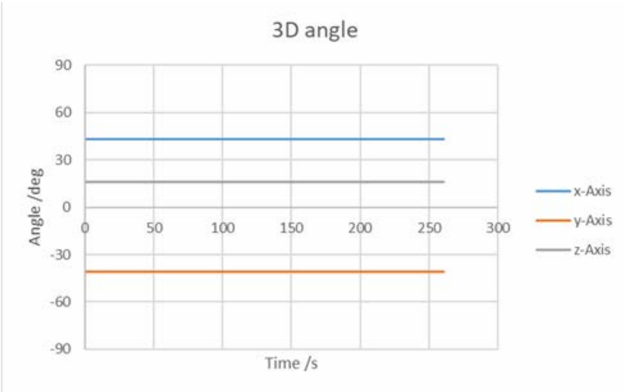

Figure 5. The 3D angle, of *x*-, *y*- and *z*-axis with respect to the gravitation field.

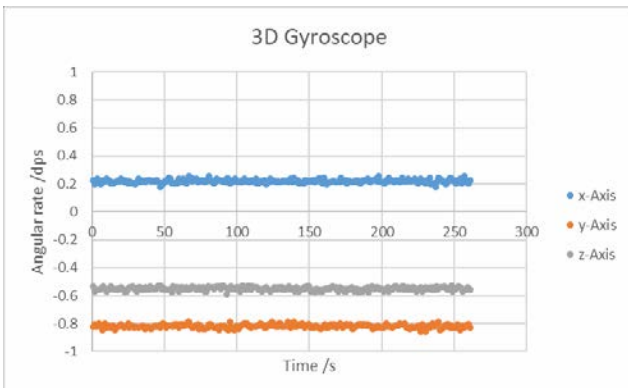

Figure 6. The 3D gyroscope, spreaded along *x*-, *y*- and *z*-axis of the IMU.

As expected in static conditions, IMU indications of both 3D gravity offsets, Figure 4, and 3D angles, Figure 5, are constant as a function of time. Namely, 3D gravity offsets are g_x=698.9±0.2 mg, g_y=-670.0±0.2 mg, and g_z 291.0±0.2 mg, and 3D angles, of *x*-, *y*- and *z*-axis with respect to the gravity axis, are 43°, -41° for *x*- and *y*-axis, and 16° for *z*-axis. Despite some systematic differences from the expected values (i.e., 45°, - 45° and 15°), presumeably due to the algorthim used for the angles calculation from the vectorial combination of g_x, g_y, and g_z, and to an intrinsic misalignement of sensitivity axes on the *x*-*y* plane (of about 6°), the indications keep constant.

On the contrary indication of 3D gyroscope (at 12.5 Hz of sampling rate, with a preimposed full scale of ±125 dps) shows values different from zero, in pure static conditions. A quite noisy angular rate is observed around the three sensitivity axes of the IMU under investigation, in particular 0.22±0.01 dps around *x*-axis, -0.82±0.01 dps around *y*-axis, and -0.55±0.01 dps around *z*-axis. This behavior is observed for all tested configurations and it can be considerd as an intrinsic systematic effect to be corrected. From experimental results the average angular rate is 0.19±0.02 dps around *x*-axis, -0.81±0.01 dps around *y*-axis, and -0.55±0.01 dps around *z*-axis. In any configuration the noise is within ±0.02. Data variability is represented by the standard deviation.

In the graph of Figure 7, the noise of the angular rate, indication of the *x*-axis, for the configuration with inclination α = 75°, at ω = 315° of rotation, is depicted.

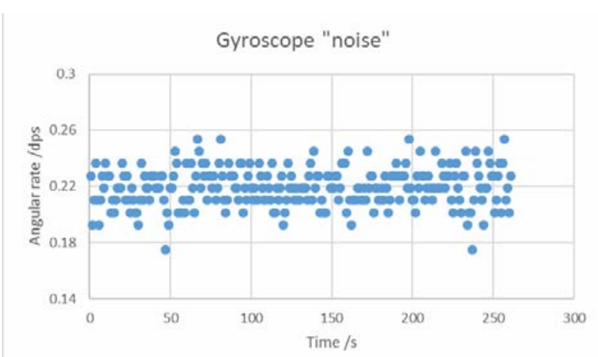

Figure 7. The noise on the indication of angular rate around *x*-axis.

Finally the IMU is subjected to a known angular rate. In this experiment the 3D gyroscope is set with 3.3 kHz of sampling rate, and ±125 dps of full scale). The IMU is mounted on the inclined planes, screwed on a stepper motor, in order to check the output in severalconfigurations, as previously described.

The stepper motor rotates the IMU from -90° and 90° at 12.0±0.1 dps. In Fig. 8, as an example, 45 s of the angular rate measurement, along *x*-axis, is depicted.

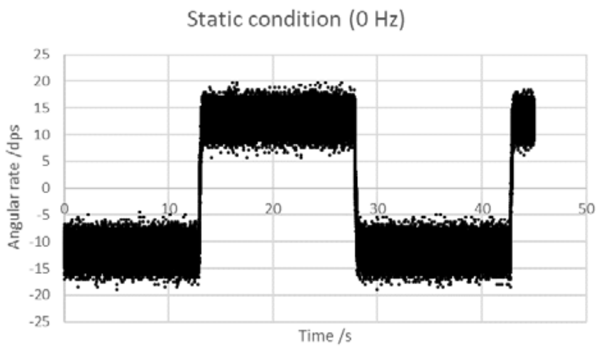

Figure 8. The 3D gyroscope *x*-axis output of the IMU at 12 dps.

In 15 s the stepper motor rotates forward form -90° to 90°, then backward form 90° to -90°, in the next 15 s.

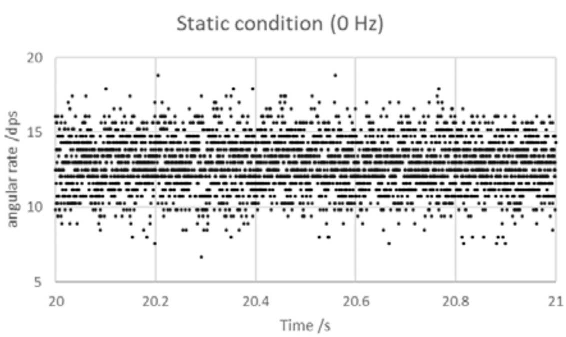

Figure 9. Data dispersion of angular rate (1 s) in static condition.

As is possible to notice from experimental evidence, the average angular rate measured around *x*-axis, is 11.8±1.7 dps (and similar range of dispersions are observed alsoaround *y*-axis and *z*-axis, namely -11.0±1.9 dps, and 4.1±1.8 dps).

B. Dynamic conditions

Once the IMU performance are determined in static conditions, the indications of 3D gyroscope are investigated in dynamic conditions, in a controlled vibrational field. The experimental set-up is shown in Fig.10. The stepper motor, on which the IMU is mounted with inclined planes, is fixed on a vibrating table (designed and realized by CENTROTECNICA s.r.l., in Masate, Italy).

Figure 10. The experimental set-up with the stepper motor on thehorizontal vibrating table.

The vibrating table allows to generate vibrations, along the perpendicular direction with respect to *g*, at very low frequency (nominally from 0 Hz up to 100 Hz), and it is addressed in particular for massive and bulky devices (up to 100 kg). The machine (Lo.F.Hi.S.) consists of an aluminum plate constrained to move only in the horizontal direction, up to the maximum velocity of 2.5 m/s, and maximum displacement of 258 mm. In this experiment a 2 Hz horizontal vibration is imposed, similar to oscillation due to car suspensions.

As it is possible to notice from Fig 11, induced vibrations do not affect the IMU angular rate indications, both in terms of average value and of data dispersion.

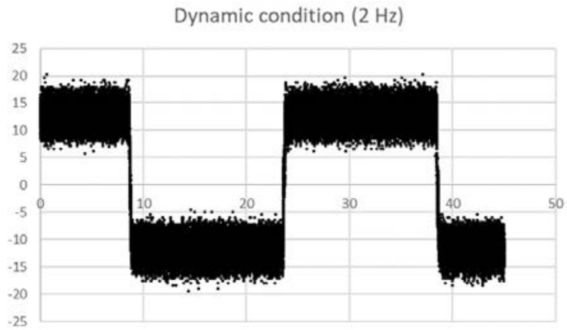

Figure 11. The 3D gyroscope *x*-axis output of the IMU at 12 dps, subjected to a 2 Hz horizontal vibration.

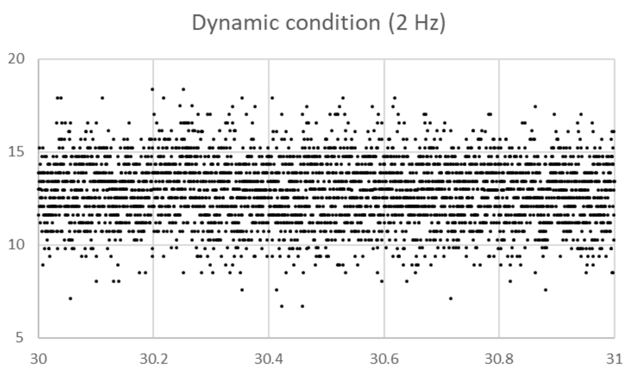

Figure 12. Data dispersion of angular rate (1 s) in dynamic conditions.

From experimental evidence, the average angular rate measured around *x*-axis, is 11.8±1.7 dps (and similar range of dispersions are observed also around *y*-axis and *z*-axis, namely -11.0±1.9 dps, and 4.1±1.8 dps), as in static condition.

V. DISCUSSION AND CONCLUSIONS

This first evidence, based on metrological characterization of the IMU’s gyroscope, in static and dynamc conditions, allows to shown the stability of the sensor and the related responsiveness. Once this behavior is known, it is possible to evaluate both the accuracy and the presision of the IMU. The accuracy can be identified from the experimental results shown in Fig. 6, in terms of systematic effects. Precision can be achieved from the known data dispersion. This is a very important evidence allowing to define the trustworthiness of the IMU. In general terms, it can be possible to summarize the IMU trustworthiness in the following graph of Fig. 13. An illustrative example the trustworthiness of *x*-axis at 12 dps, subjected to a dynamic oscillation of 2 Hz, is shown. Similar results are obtained for both *y*-axis and *z*-axis.

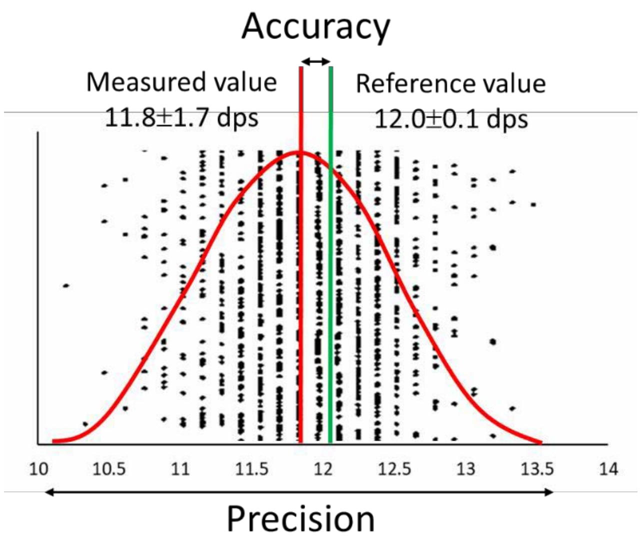

Figure 13. Trustwothiness of the 3D gyroscope *x*-axis output of the IMU at 12 dps, subjected to a 2 Hz horizontal vibration.

REFERENCES

[1] Kalra, Nidhi, and Susan M. Paddock. "Driving to safety: Howmany miles of driving would it take to demonstrate autonomous vehicle reliability?." Transportation Research Part A: Policy and Practice 94 (2016): 182-193.

[2] Holland, R., et al. "Performance testing for sensors in connected and autonomous vehicles: feasibility studies. Appendices." (2020).

[3] https://www.europarl.europa.eu/news/en/press- room/20170227IPR64173/boosting-innovation-fairness-sustainability- and-safety-in-road-transport.

[4] https://unece.org/sustainable-mobility-and-smart-connectivity

[5] JCGM 200 International Vocabulary of Metrology Basic and General Concepts and Associated Terms (VIM 3rd Edition) (France: Joint Committeefor Guidesin Metrology, Sévres), 2012.

[6] Milton, M.J.T., Possolo, A. Trustworthy data underpin reproducible research. Nat. Phys. 16, 117–119 (2020). https://doi.org/10.1038/s41567-019-0780-5

[7] A. Prato, F. Mazzoleni, and A. Schiavi, "Traceability of digital 3-axis MEMS accelerometer: simultaneous determination of main and transverse sensitivities in the frequency domain," Metrologia, 57(3), p. 035013, 2020.

[8] Prato, A., Mazzoleni, F., & Schiavi, A. (2020). Evaluation and correction of systematic effects in a simultaneous 3-axis vibration calibration system. ACTA IMEKO, 9(5), 388-393.

[9] https://www.st.com/resource/en/datasheet/lsm6dsr.pdf (Last access 30 November 2020)

[10] https://www.st.com/resource/en/data_brief/32f769idiscovery.pdf (Last access 30 November 2020)

[11] A. Prato, N. Montali, C. Guglielmone and A. Schiavi, " Pressure calibration of a digital microelectromechanical system microphone by comparison," The Journal of the Acoustical Society of America 144, EL297, 2018.

[12] A. Prato, F. Mazzoleni, and A. Schiavi, "Metrological traceability for digital sensors in smart manufacturing: calibration of MEMS accelerometers and microphones at INRiM," In 2019 II Workshop on Metrology for Industry 4.0 and IoT (MetroInd4. 0&IoT) (pp. 371-375). IEEE.

[13] A. Prato, A. Schiavi, F. Mazzoleni, A. Touré, G. Genta, M. Galetto, "A reliable sampling method to reduce large set of measurements: a case study on calibration of digital 3-axis MEMSaccelerometers" 2020 IEEE International Workshop on Metrology for Industry 4.0 and IoT.

[14] Schiavi, A., Prato, A., Mazzoleni, F., D'Emilia, G., Gaspari, A., & Natale, E. (2020, June). Calibration of digital 3-axis MEMS accelerometers: A double-blind «multi-bilateral» comparison. In 2020 IEEE International Workshop on Metrology for Industry 4.0 & IoT (pp. 542-547). IEEE.

[15] M. Galetto, A. Schiavi, G. Genta, A. Prato and F. Mazzoleni, "Uncertainty evaluation in calibration of low-cost digital MEMS accelerometers for advanced manufacturing applications," CIRP Annals 68, 535-538, 2019.

[16] Geist J, Afridi M Y, McGray C and Gaitan M 2017 Gravity-based characterization of three-axis accelerometers in terms of intrinsic accelerometer parameters J. Res. Natl Inst. Stand. Technol. 122 1–14

[17] Gaitan, M., Bautista, I. M. L., & Geist, J. (2021). Reduction of calibration uncertainty due to mounting of three-axis accelerometers using the intrinsic properties model. Metrologia, 58(3), 035006.